RSC Advances

PAPER

View Article Online
View Journal | View Issue

Cite this: *RSC Adv.*, 2020, **10**, 4023

Catalytic and photocatalytic oxidation of diphenyl sulphide to diphenyl sulfoxide over titanium dioxide doped with vanadium, zinc, and tin

Marcelina Radko,[a] Andrzej Kowalczyk,[a] Paweł Mikrut,[a] Stefan Witkowski,[a] Włodzimierz Mozgawa,[b] Wojciech Macyk[a] and Lucjan Chmielarz*[a]

Received 26th November 2019
Accepted 19th January 2020

DOI: 10.1039/c9ra09903d

rsc.li/rsc-advances

Samples of TiO_2 (P25) doped with zinc, tin, and vanadium, thermally treated at 550 °C for 6 h, were tested as catalysts and photocatalysts for the oxidation of diphenyl sulphide to diphenyl sulfoxide and sulfone, using hydrogen peroxide as an oxidation agent. Thermal treatment of pure TiO_2 and its vanadium-doped forms resulted in a decrease of anatase and an increase of rutile content. The opposite effect was observed for TiO_2 doped with zinc or tin, where thermal treatment resulted in the rutile to anatase phase transition. The role of V, Zn, and Sn admixtures as TiO_2 phase-composition controllers was postulated. The catalytic and photocatalytic activity was found to be influenced more by the rutile and anatase contents of the samples than the presence of admixtures. The rutile-containing samples, TiO_2 and V-TiO_2, presented much better activity in the catalytic oxidation of diphenyl sulphide compared with the catalysts that only contained the anatase phase, Sn-TiO_2 and Zn-TiO_2. The reaction efficiency was significantly improved under UV radiation. In this case, the best photocatalytic activity was found for calcined TiO_2, containing both anatase and rutile components. An increase in rutile content, observed in the vanadium-doped TiO_2, decreased the efficiency of the photocatalytic diphenyl sulphide oxidation. Thus, the presence of both anatase and rutile phases, with their favourable contributions, typical for P25, is necessary for the effective oxidation of Ph_2S to Ph_2SO. Moreover, it was shown that for the second oxidation stage, Ph_2SO to Ph_2SO_2, the presence of the rutile phase is very important.

Introduction

Selective oxidation of organic sulphides to sulfoxides is one of the key reactions in organic chemistry. The organic sulfoxides, obtained in such a process, are important chemicals in many branches of chemical industry, including, among others, drug synthesis. A broad range of various oxidants for the selective synthesis of sulfoxides have been proposed. Among them $KMnO_4$, HNO_3, RuO_4, $NaIO_4$, and MnO_2 were reported as effective oxidation agents for the selective oxidation of organic sulphides.[1,2] However, in the case of using such oxidants, equimolar amounts of deoxygenated compounds, including heavy metals, are formed as waste products.[3,4] To overcome these undesired effects of conventional oxidants, hydrogen peroxide can be used as an oxidation agent. In this case the only product of H_2O_2 decomposition is H_2O. Many authors, such as Shaabani *et al.*,[5] Golchoubian *et al.*,[6] Sato *et al.*,[7] and Noyori *et al.*,[8] reported hydrogen peroxide as a very promising oxidant in various reactions that transform organic compounds. Hydrogen peroxide is also very promising for application on an industrial scale due to its low production cost, safety in storage, transportation, and operation. Thus, using hydrogen peroxide as an oxidation agent is beneficial from both an environmental and economic point of view.

We focus on Ph_2S oxidation using bare titanium dioxide (P25) or metal-doped TiO_2 as a catalyst. Titanium dioxide, in addition to its good catalytic properties, is an effective photocatalyst in various reactions, such as the oxidation of organic compounds. TiO_2 is widely used as a photocatalytic material because of its strong oxidising ability, high physical and chemical stability, nontoxicity, low cost, and high availability.[9,10] Recently, titanium dioxide has been used in solar cells, thin film optical devices, or as a gas sensor.[11] Moreover, titanium dioxide may be used in the environmental remediation of toxic or harmful compounds by converting them to harmless products *via* a photooxidation process.[12]

In this study, we use bare titanium dioxide (commercial P25) and vanadium-, tin-, or zinc-doped TiO_2 samples as catalysts and photocatalysts. Titanium dioxide modified with metal ions was used and verified as an effective catalyst and photocatalyst in the oxidation of Ph_2S. Reference TiO_2 and metal loaded TiO_2 powders have different crystal structures. The ratio between anatase and rutile phases influences the catalytic and

[a]*Faculty of Chemistry, Jagiellonian University, Gronostajowa 2, 30-387 Kraków, Poland. E-mail: chmielar@chemia.uj.edu.pl; Tel: +48 12 6862417*
[b]*Faculty of Materials Science and Ceramics, AGH University of Science and Technology, Mickiewicza 30, 30-059 Kraków, Poland*

photocatalytic activity of these materials in Ph_2S oxidation. Bettinelli *et al.*[12] reported that the crystal structure, surface area, crystallinity, and porosity of TiO_2 materials, affect the photocatalytic activity of TiO_2. It was noticed by Bettinelli *et al.*,[12] Litter *et al.*,[13] and Wilke *et al.*[14] that the incorporation of transition metals (V, Fe, Ru, Mn, or Au) as dopants into TiO_2 may shift the photocatalytic activity of the material toward the visible light spectral range. Several papers[15,16] have shown that vanadium as a TiO_2 dopant increases photocatalytic activity of titanium. However, some authors observed the opposite effect when incorporating vanadium, a slight decrease in the TiO_2 activity upon doping with vanadium.[17,18] These significant differences may result from different doping methods and the resulting phase composition of the V-TiO_2 materials. Various experimental parameters in the preparation of metal-doped TiO_2 can strongly influence the photoactivity of the synthesised samples.[19] It was also reported that the photocatalytic activity of TiO_2 strongly depends on the amount of metals used as dopants.[19,20] Additionally, the use of metal ions with the same or a smaller ionic radius than titanium(IV) seems to be crucial. The substitution of dopant ions into the framework of titanium dioxide may decrease the band gap energy of such materials and therefore increase their visible light induced photoactivity.[21] Moreover, the role of anatase and rutile phases in the Ph_2S to Ph_2SO and Ph_2SO to Ph_2SO_2 oxidation steps in the dark and under UV irradiation is another important issue that is discussed in this study.

Experimental

Materials

The following chemicals were used in the studies: titanium(IV) oxide (Aeroxide P25, >99.5%, Acros Organics), ammonium metavanadate (100%, Merck Millipore), zinc chloride (≥98%, Honeywell Fluka), tin(II) chloride dehydrate (98%, Honeywell Fluka), acetonitrile (99.8%, Aldrich), bromobenzene (>99.5%, Aldrich), diphenyl sulphide (98%, Aldrich) and hydrogen peroxide (30%, POCh).

Catalyst preparation

Titanium-supported vanadium, zinc, and tin catalysts were prepared by incipient wetness impregnation. The samples with the intended metal content of 0.1 wt% were obtained by soaking the commercial titanium dioxide powder (P25) with an aqueous solution of suitable metal salts: ammonium metavanadate, zinc chloride, and tin(II) chloride dehydrate. The volume of the solutions used for impregnation was equal to the water sorption capacity of P25. The samples that were soaked with metal salt solutions, were closed in vessels and stirred for 2 h using a roller mixer. Then, the samples were dried overnight and finally calcined at 550 °C for 6 h (the temperature was increased from room temperature to 550 °C at a rate of 1 °C min^{-1} and then for the isothermal calcination step the temperature was held at 550 °C for 6 h).

Catalysts characterisation

The vanadium content in the samples was analysed using the Inductively Coupled Plasma-Optical Emission Spectrometry (ICP-OES) method. Firstly, 100 mg of the sample was dissolved in a mixture of 8 cm^3 HCl (30%), 2 cm^3 HNO_3 (67%), and 1 cm^3 HF (50%) at 190 °C using an advanced microwave digestion system (Ethos Easy, Milestone). The obtained solutions were then analysed with respect to the deposited metal content using an ICP-OES instrument (iCAP 7400, Thermo Science).

The phase composition and crystal size of the samples were studied using X-ray diffraction (XRD) using a Brucker D2 diffractometer. The measurements were performed using Cu-Kα radiation in the 2 theta range of 20–80° with a step of 0.02°.

Moreover, to determine the crystallographic forms of TiO_2, anatase, and rutile, Raman spectroscopic analysis was applied. Raman spectra were obtained using a HORIBA Jobin Yvon LabRAM HR micro Raman spectrometer. A 532 nm diode Nd:YAG laser along with 1800 diffraction grating and 100× Olympus objective were used. The laser power was adjusted to approximately 9 mW. Two scans of 11 s each were taken.

Textural parameters of the samples were determined by N_2 adsorption at −196 °C using a 3Flex (Micrometrics) automated gas adsorption system. Prior to the measurement the samples were outgassed under vacuum at 350 °C for 24 h.

The UV-vis diffuse reflectance spectra of the samples were measured at room temperature using an Evolution 600 (Thermo) spectrophotometer. The spectra were recorded in the range of 190–900 nm with a resolution of 4 nm. The bandgap energy was estimated from the Tauc plot, $(F(R)\cdot h\nu)^{1/2}$ *vs.* $h\nu$, where $F(R) = (1 - R)^2/R$ is the Kubelka–Munk function.

Catalytic and photocatalytic studies

The samples of TiO_2 (P25) doped with zinc, tin, or vanadium were tested as catalysts and photocatalysts for the oxidation of diphenyl sulphide (Ph_2S) to diphenyl sulfoxide (Ph_2SO) and sulfone (Ph_2SO_2) using hydrogen peroxide as oxidation agent. The reaction was performed in a 100 cm^3 round-bottom flask equipped with a stirrer, dropping funnel, and thermometer. The reaction mixture consisted of 2 cm^3 (0.4 mmol) of diphenyl sulphide, 20 cm^3 of acetonitrile as a solvent, 0.01 cm^3 (0.1 mmol) of bromobenzene as an internal standard, and 25 mg of the catalyst. The obtained mixture was stirred (1000 rpm) at 25 °C for 10 min and then 0.06 cm^3 (2 mmol) of 30% hydrogen peroxide was added. For the catalytic studies, the reaction was performed in the dark in order to avoid the photocatalytic conversion of Ph_2S (conditions marked here as "in dark"). Moreover, the reaction was also performed under UV radiation (marked as "under light"). In this case, a 150 W xenon short arc lamp was used as a UV light source (11.65 mW cm^{-2}). To avoid the excitation of Ph_2S and its direct photooxidation, a 320 nm cut off filter was applied, as well as a NIR and IR filter (10 cm optical path, 0.1 mol dm^{-3} solution of $CuSO_4$). The progress of the reaction was monitored by analysing the reaction mixture using the High Performance Liquid Chromatography (HPLC) method using a mixture of acetonitrile/water as the eluent with the volume ratio of 80 : 20. Samples of the reaction mixture

were taken at regular intervals: every 10 min within the first hour and every 30 min afterwards. The samples were filtered through the 0.22 μm nylon membrane filter and analysed using the PerkinElmer Flexar chromatograph equipped with the analytical C18 column (150 mm × 4.6 mm i.d., 5 μm pore size). The column was maintained at 25 °C throughout analysis and the UV detector was set at 254 nm.

Leaching of the deposited metal species from P25 was studied for the selected catalysts by the chemical analysis of the reaction mixture after it was separated from the solid catalyst using the ICP-OES method (iCAP7400, Thermo Science). Moreover, in order to check the catalytic activity of the metal species leached from the solid catalyst, fresh reactants (H_2O_2 and Ph_2S) were added into the solution after it was separated from the catalyst and then the catalytic test was continued for a further 4 h. It was shown that the amount of metal leached was below 5 wt% of its initial content in the sample. Moreover, the conversion of Ph_2S was not detected for the reaction conducted in solution after the separation from the solid catalysts.

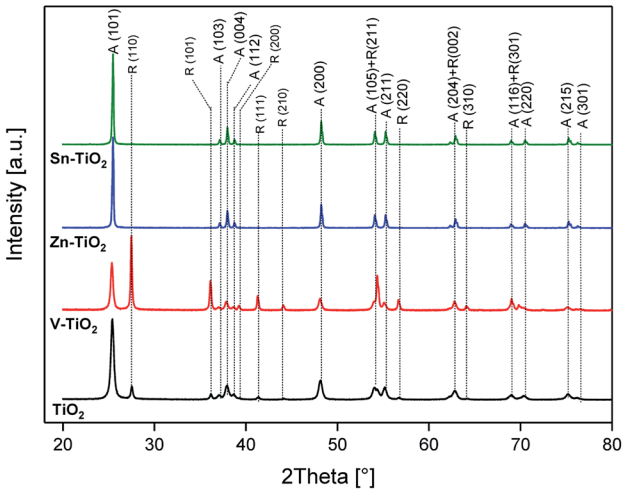

Fig. 1 X-ray diffraction patterns of TiO_2 (P25) and its modifications with vanadium, zinc and tin.

Results and discussion

The chemical compositions and textural parameters of the studied catalysts are presented in Table 1. It can be seen that the real content of the metals deposited on the P25 surface is relatively close to the expected value of 0.1 wt%. The specific surface area (SSA) of the samples is in the range of 9–38 $m^2\ g^{-1}$. It should be noted that all samples, including unmodified TiO_2, were calcined at 550 °C for 6 h. The SSA of the non-calcined P25 was about 40 $m^2\ g^{-1}$. It can be seen that calcination resulted in a significant decrease in the SSA. In the case of calcined TiO_2 the most pronounced decrease in the SSA, to 9 $m^2\ g^{-1}$, was observed. For the samples modified with metals the decrease in the SSA, especially for V-TiO_2, was less pronounced. A similar tendency was observed for the pore volumes of the studied samples. Thus, it seems that the deposition of metals influenced the process of TiO_2 sintering. A similar effect was reported and discussed in our previous paper for TiO_2 doped with vanadium.[22]

The phase composition of the samples was analysed using X-ray diffraction and Raman spectroscopy. The results of these analyses are presented in Fig. 1 and 2, respectively. The diffractogram recorded for TiO_2 (P25 calcined at 550 °C) encompasses reflections characteristic of anatase and rutile phases. We used MAUD software for Rietveld analysis[23] to refine the anatase and rutile content, the results showed that the anatase and rutile content in the TiO_2 sample were 87 to 13%, with average crystallite sizes of 36 and 45 nm, respectively. The introduction of small amounts of vanadium into TiO_2 followed by its calcination at 550 °C (V-TiO_2) resulted in a significant decrease in the anatase and an increase in the rutile content. In this case, the anatase and rutile contents, determined by the Rietveld method, were about 45 to 55%, with average crystallite sizes of about 45 and 115 nm, respectively. The effect of the anatase to rutile transformation in the vanadium-doped TiO_2 was confirmed by Raman analysis of the samples (Fig. 2). Calcination of the V-TiO_2 samples resulted in the appearance of the bands characteristic for the rutile phase at 234, 449, and 612 cm^{-1}.[24] For the calcined TiO_2 sample, these bands are significantly less intense or even invisible. A similar effect of the anatase to rutile transformation in the presence of small amounts of vanadium was recently reported by Shao *et al.*,[25] as well as in our previous paper.[22] This phenomenon could be explained by the possible incorporation of V^{4+} cations into the vacant Ti^{4+} positions in anatase.[26,27] Such a substitution is possible due to the similar ionic radii of Ti^{4+} (0.061 nm) and V^{4+} (0.058 nm).[27] Moreover, the same valence of these cations results in the electroneutrality of the anatase lattice. Thus, it seems possible that the incorporation of V^{4+} into the anatase lattice acts as initiation nuclei for the anatase to rutile phase transformation.[28] The opposite effect was observed for TiO_2 doped with zinc or tin, where the calcination of such samples resulted in the disappearance of the reflections characteristic of rutile (Fig. 1). In the case of TiO_2 doped with tin or zinc, only the

Table 1 Content of the deposited metals and textural parameters of the TiO_2 based samples

Sample	Metal content/wt%	BET surface area/$m^2\ g^{-1}$	Pore volume/$cm^3\ g^{-1}$
TiO_2	—	9	0.028
Zn-TiO_2	0.098 (Zn)	12	0.031
Sn-TiO_2	0.065 (Sn)	12	0.034
V-TiO_2	0.073 (V)	38	0.266

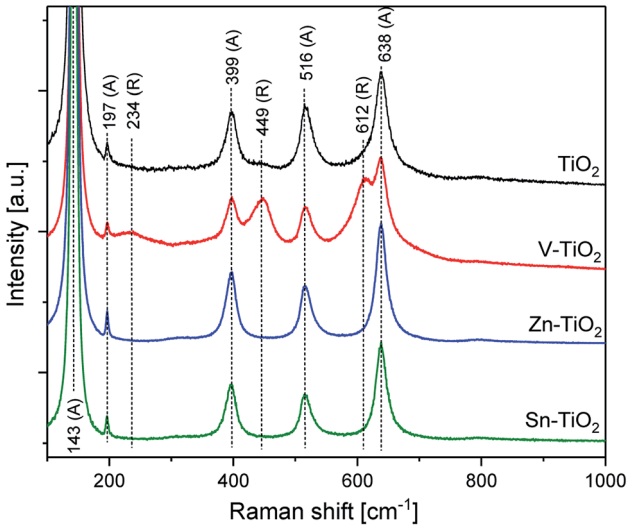

Fig. 2 Raman spectra of TiO_2 (P25) and its modifications with vanadium, zinc, or tin.

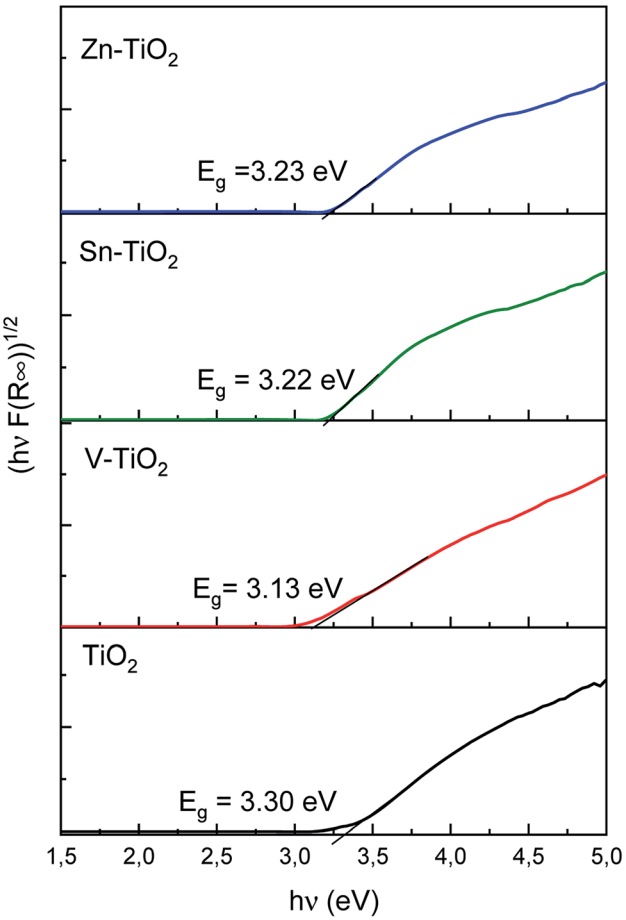

Fig. 3 Band gap energies of pure and metal-doped TiO_2 (P25).

reflections characteristic of the anatase phase were identified. For both samples, the average anatase crystal size was very similar (44–45 nm). The results of the XRD analysis are fully consistent with the results of Raman analysis of the Sn-TiO_2 and Zn-TiO_2 samples. The spectra recorded for these samples only contain bands characteristic of anatase located at 143, 197, 399, 516, and 638 cm^{-1} (Fig. 2).[24] Thus, the obtained results clearly show that doping of titanium with small amounts of zinc or tin inhibits the transformation of anatase to rutile. In contrast to V^{4+} (0.058 nm), the ionic radii of Zn^{2+} (0.074 nm) and Sn^{4+} (0.069 nm) are too large to substitute Ti^{4+} (0.061 nm) in the anatase lattice and therefore the initiation of the anatase to rutile phase transformation based on this mechanism is not possible. Sangchay[29] reported that depending on the SnO_2 content in TiO_2, various contributions of rutile were achieved upon the thermal treatment of the samples at 700 °C. In the case of the samples with a low SnO_2 loading (1 wt%), the formation of rutile was not observed and small amounts of the rutile phase even disappeared. For the samples with a higher SnO_2 content a partial transformation of anatase to rutile was observed.

Titanium doped with vanadium, tin, or zinc was tested as a catalyst and photocatalyst for diphenyl sulphide (Ph_2S) oxidation to diphenyl sulfoxide (Ph_2SO) and sulfone (Ph_2SO_2), using H_2O_2 as the oxidant. Ph_2SO and Ph_2SO_2 were the only detected products of Ph_2S oxidation, therefore only selectivity to Ph_2SO is shown in the figures. The selectivity to Ph_2SO_2 can be calculated by subtracting the selectivity of Ph_2SO from 100%.

In the preliminary catalytic and photocatalytic tests that were conducted in the absence of H_2O_2 for the calcined TiO_2 sample, no Ph_2S conversion was observed during the 3 h of the tests (results not shown). This shows that the oxidation of diphenyl sulphide cannot be achieved in the absence of hydrogen peroxide, even in the presence of oxygen from the air. Other catalytic and photocatalytic tests were performed in the presence of H_2O_2 as the oxidant. The results of Ph_2S oxidation in the presence of bare TiO_2 sample are presented in Fig. 4. The conversion of diphenyl sulphide in the dark is significantly lower compared with that observed under illumination. These results clearly show that the catalytic conversion of Ph_2S in the presence of TiO_2 is feasible as a thermal catalytic process, however, the efficiency of the reaction is significantly intensified when it is performed as a light assisted process. This is not surprising if we take into account the fact that P25 TiO_2 is a very efficient photocatalyst of various reactions involving oxygen and hydrogen peroxide activation.[30] It should be noted that the Ph_2S conversion reached 100% after 30 min of the photocatalytic process. However, a simultaneous conversion of diphenyl sulphide to both reaction products, Ph_2SO and Ph_2SO_2, is a serious problem in terms of commercial applications. Therefore, one of the main goals of this study was to develop a catalyst with a high selectivity for the specific reaction product.

The results of the catalytic and photocatalytic studies for the V-TiO_2 sample are presented in Fig. 5. In this case, the Ph_2S conversion in the dark increased gradually during the reaction time, reaching nearly 60% after 3 h of the catalytic test. The selectivity to Ph_2SO significantly decreased during the reaction run, starting from 96% at the beginning of the experiment and decreasing to about 58% after 3 h. In the case of the light

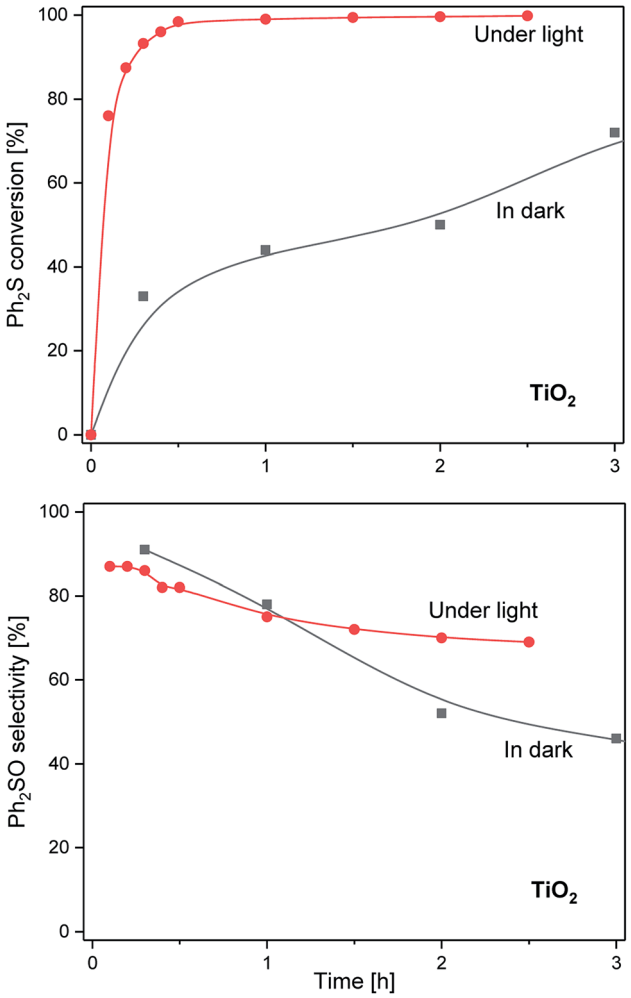

Fig. 4 Results of catalytic (in dark) and photocatalytic (under light) diphenyl sulphide oxidation by H_2O_2 in the presence of TiO_2. Diphenyl sulphide conversion (top) and diphenyl sulfoxide selectivity (bottom).

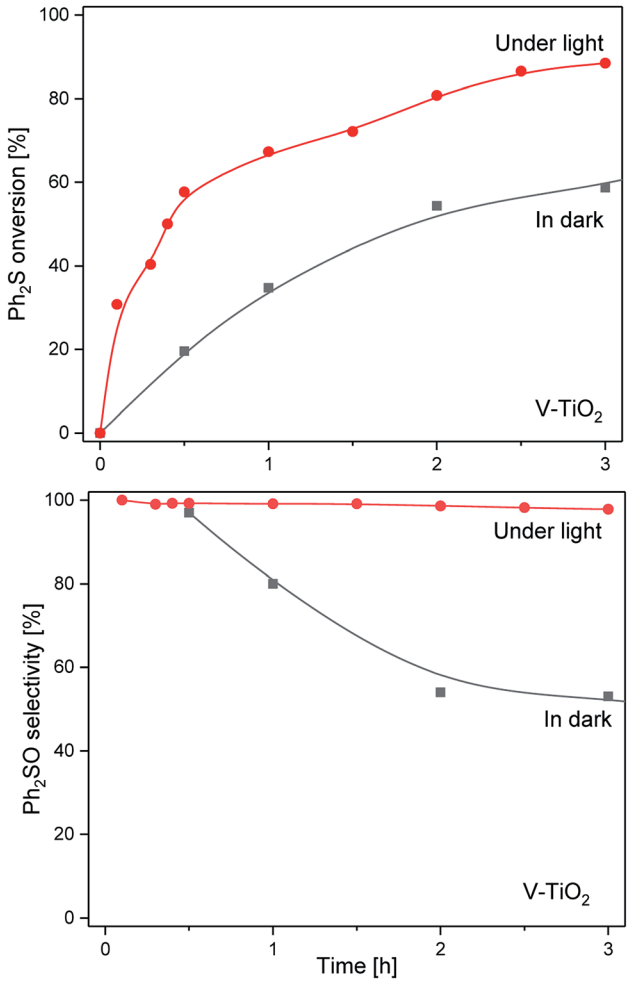

Fig. 5 Results of catalytic (in dark) and photocatalytic (under light) diphenyl sulphide oxidation by H_2O_2 in the presence of the V-TiO_2 sample. Diphenyl sulphide conversion (top) and diphenyl sulfoxide selectivity (bottom).

assisted reaction, an increase of the Ph_2S conversion by 30–40% in comparison with the experiment in the dark was observed. After 3 h the Ph_2S conversion did not exceeded 90% with the selectivity to Ph_2SO of about 98%. Thus, the photocatalytic activity of V-TiO_2 was lower than that of bare TiO_2, but the selectivity to Ph_2SO was significantly improved.

Fig. 6 presents the results of the catalytic and photocatalytic studies on TiO_2 modified with zinc (Zn-TiO_2). The Ph_2S conversion in the dark reached about 10% after 1 h and remained at this level for the next 2 h. Thus, the catalytic activity was significantly lower compared with TiO_2 and V-TiO_2. The selectivity to Ph_2SO was in the range of 77–86% and decreased slightly during the reaction run. In the case of the light assisted reaction, a much higher Ph_2S conversion, in comparison with the reaction in the dark, was obtained in the presence of the Zn-TiO_2 catalyst. The complete Ph_2S conversion was observed after 2 h of irradiation. In contrast to bare TiO_2, using Zn-TiO_2 as a catalyst resulted in the oxidation of diphenyl sulphide nearly exclusively to diphenyl sulfoxide. Selectivity towards Ph_2SO dropped insignificantly from the 100% observed after 2 h to 98% which was measured after 3 h of the photocatalytic process. Thus, Zn-TiO_2 was found to be less active in the photocatalytic conversion of Ph_2S compared with bare TiO_2, but more active than V-TiO_2. However, what is important is that the Zn-TiO_2 material showed a much higher selectivity in the conversion of Ph_2S to Ph_2SO compared with TiO_2 and V-TiO_2.

The Sn-TiO_2 catalyst showed a slightly higher activity in the dark (Fig. 7) than Zn-TiO_2. The Ph_2S conversion reached *ca.* 20% after 1 h and remained at this level for the next 2 h. It means, that the diphenyl sulphide conversion was about two times higher than that observed for Zn-TiO_2. The selectivity to Ph_2SO was in the range of 67–77% with only slight fluctuations during the reaction. In the case of the light assisted process, the Ph_2S conversion was significantly higher and reached 100% after 2.5 h. The selectivity to Ph_2SO was particularly high, but it dropped from 99% (after 1.5 h) to 91% during the next 90 min of irradiation.

The comparison of the presented results shows the important influence of the incorporated metal additives, even in very small amounts, on the catalytic and photocatalytic properties of

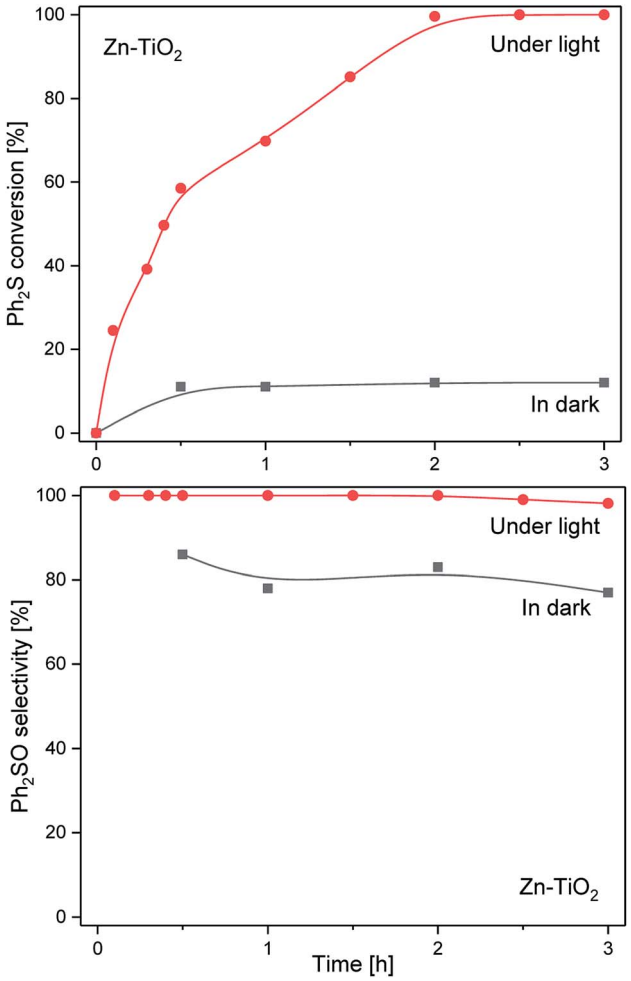

Fig. 6 Results of catalytic (in dark) and photocatalytic (under light) diphenyl sulphide oxidation by H_2O_2 in the presence of the Zn-TiO_2 sample. Diphenyl sulphide conversion (top) and diphenyl sulfoxide selectivity (bottom).

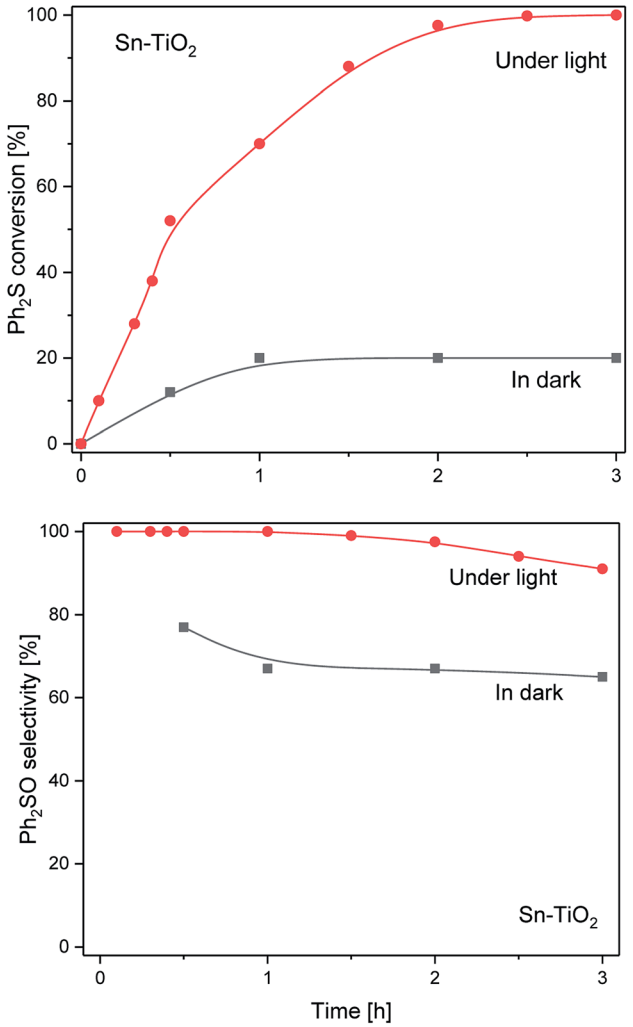

Fig. 7 Results of catalytic (in dark) and photocatalytic (under light) diphenyl sulphide oxidation by H_2O_2 in the presence of the Sn-TiO_2 sample. Diphenyl sulphide conversion (top) and diphenyl sulfoxide selectivity (bottom).

titanium dioxide. The analysis of the results of the conversion of diphenyl sulphide and selectivity towards diphenyl sulfoxide shows that the photocatalytic reaction is a much more effective approach for the production of Ph_2SO compared with the thermal catalytic reaction. Of all the materials in this study, Zn-TiO_2 is the most promising catalyst, as it allowed the complete and exclusive conversion of diphenyl sulphide to diphenyl sulfoxide. Further efforts will be made to optimise the zinc content and the procedure of catalyst synthesis. Also, further studies are required to elucidate the role of dopants; however, taking into account our recent findings we assume, that a reasonable explanation of the role of V, Zn, and Sn admixtures is their function as phase composition controllers.[31]

For the V-TiO_2 sample, in contrast to the other studied catalysts, a complete conversion of diphenyl sulfoxide was not obtained in the photocatalytic test. This could be related to the fast decomposition of H_2O_2 over V-TiO_2, and therefore a limited efficiency of Ph_2S oxidation due to the lack of an oxidising agent. Since V-TiO_2 contains the highest amount of rutile-TiO_2, the decomposition of hydrogen peroxide can be attributed to the efficient reduction of hydrogen peroxide, as demonstrated for various rutile and anatase samples.[32] To verify this hypothesis a further photocatalytic test was carried out, in which an additional portion of H_2O_2 was added after 2.5 h of the reaction. This action did not result in any significant changes in the Ph_2S conversion and selectivity profiles (Fig. 8). Thus, it seems that a relatively low Ph_2S conversion observed in the presence of the V-TiO_2 catalyst is not related to the limited accessibility of H_2O_2 in the reaction mixture during the catalytic test.

Analysis of the presented results raises questions regarding the source of different efficiencies of the Ph_2S conversion in the dark and upon irradiation and the source of different catalytic and photocatalytic performances of the studied catalysts.

The mechanisms of photocatalytic reactions over TiO_2 have been studied for last five decades.[30,33,34] Upon TiO_2 excitation, photogenerated holes and electrons can participate in the oxidation and reduction reactions. In particular, hydrogen peroxide can either be oxidised or reduced:

$$H_2O_2 + h^+ \rightarrow HO_2^{\bullet} + H^+ \quad (1)$$

$$H_2O_2 + e^- \rightarrow HO^{\bullet} + OH^- \quad (2)$$

Photogenerated electrons may also react with oxygen molecules with the formation of superoxide radical anions:

$$O_2 + e^- \rightarrow O_2^{\bullet -} \quad (3)$$

Valence band holes oxidise water molecules or hydroxyl groups yielding hydroxyl radicals:

$$H_2O + h^+ \rightarrow H^+ + HO^{\bullet} \quad (4)$$

$$OH^- + h^+ \rightarrow HO^{\bullet} \quad (5)$$

Among the generated species, the hydroxyl radicals and superoxide radical ions can play a key role in oxidation of diphenyl sulphide. Upon illumination ($\lambda > 320$ nm) the studied materials may generate hydroxyl radicals and superoxide ions. The question arises whether both $HO^{\bullet}$ and $O_2^{\bullet -}$ participate in the process of diphenyl sulphide oxidation. To further understand the mechanism, *tert*-butyl alcohol (*t*-BuOH), which is a hydroxyl radical scavenger, was added to the reaction mixture. The results of this experiment for the calcined TiO_2 sample, presented in Fig. 9, show that elimination of hydroxyl radicals from the reaction mixture significantly decreased the diphenyl sulphide conversion, compared with the reaction in the absence of *t*-BuOH. Thus, it can be concluded that hydroxyl radicals play a significant role in diphenyl sulphide oxidation. On the other hand, the elimination of hydroxyl radicals from the reaction mixture did not completely suppress the diphenyl sulphide conversion, thus it seems that both hydroxyl radicals and superoxides are indispensable in the process. Elimination of the hydroxyl radicals significantly decreases the selectivity of the reaction to Ph_2SO and increases the selectivity to the over-oxidised product, Ph_2SO_2. However, a similar effect was observed for the dark reaction (data not shown). Therefore, the adsorption of reactants competing with adsorption of the *t*-BuOH may play a certain role. Also, $O_2^{\bullet -}$ ions could be more effective than the hydroxyl radicals in the oxidation of Ph_2S to Ph_2SO_2. There are also studies on the photocatalytic Ph_2S oxidation to Ph_2SO governed by oxidation with a superoxide.[35] Due to its apparent complexity and the involvement of both photoinduced and thermal processes, a detailed analysis of the mechanism will be the scope of further studies. For all the studied catalysts, a decrease in the selectivity to Ph_2SO and an increase in the selectivity to Ph_2SO_2 were observed for the tests conducted in the dark and upon irradiation. In the case of the materials consisting of both anatase and rutile forms (bare TiO_2 and V-TiO_2) the dark conversion of Ph_2S was significantly more efficient compared with that catalysed by anatase-based semiconductors (Sn-TiO_2 and Zn-TiO_2). Anatase/rutile composites mostly promoted the production of Ph_2SO_2. On the other hand, reactions catalysed by anatase materials mostly led to the production of Ph_2SO. These results point at a specific interplay between anatase and rutile, which results in the enhanced selective production of Ph_2SO_2 in the dark. This effect disappears under UV irradiation, when Ph_2SO was produced almost exclusively. Synthesis of Ph_2SO_2 under photocatalytic conditions was observed only after the complete conversion of Ph_2S to Ph_2SO. This suggests that the oxidation of Ph_2S to Ph_2SO_2 is a two-step reaction, involving Ph_2SO as an intermediate. At this stage, however, the direct oxidation of Ph_2S to Ph_2SO_2 cannot be excluded. To recognise the efficiency of both possible reaction steps, the catalytic oxidation of the intermediate reaction product, Ph_2SO, to the final product, Ph_2SO_2, was tested in the dark and upon irradiation. The results of these studies, presented in Fig. 10, are striking. In the case of the two most active catalysts, TiO_2 and V-TiO_2, the efficiency of the oxidation of Ph_2SO to Ph_2SO_2 was significantly higher in the dark, while for the other two samples, Sn-TiO_2 and Zn-TiO_2, the results obtained in the dark and under irradiation were much worse. Thus, it seems that UV irradiation does not accelerate the oxidation of Ph_2SO to Ph_2SO_2, but in fact it even hinders it. This observation corresponds to the results of diphenyl oxidation presented in Fig. 3–6, where selectivity of the Ph_2S conversion to Ph_2SO_2 was much higher in the dark. In the case of all the studied samples, it seems that the first stage of diphenyl sulphide oxidation, $Ph_2S \rightarrow Ph_2SO$, is UV sensitive, while the second oxidation stage, $Ph_2SO \rightarrow Ph_2SO_2$, is not. Apparently, photoinduced reactive oxygen species do not facilitate this reaction. This is another argument against the oxidation of Ph_2SO to Ph_2SO_2 by hydroxyl radicals.

The differences in catalytic and photocatalytic performance of the studied samples are also intriguing. TiO_2 was doped with very small amounts of vanadium, tin, or zinc, and then calcined at 550 °C for 6 h. During calcination, there were significant changes in the phase composition of the samples. As shown by XRD (Fig. 2) and Raman spectroscopy (Fig. 3), in the case of V-TiO_2 the contribution of rutile significantly increased compared with calcined pure TiO_2, while the opposite effect was found for Sn-TiO_2 and Zn-TiO_2, where rutile present in the starting TiO_2 (P25) material disappeared. Thus, the TiO_2 and V-TiO_2 samples

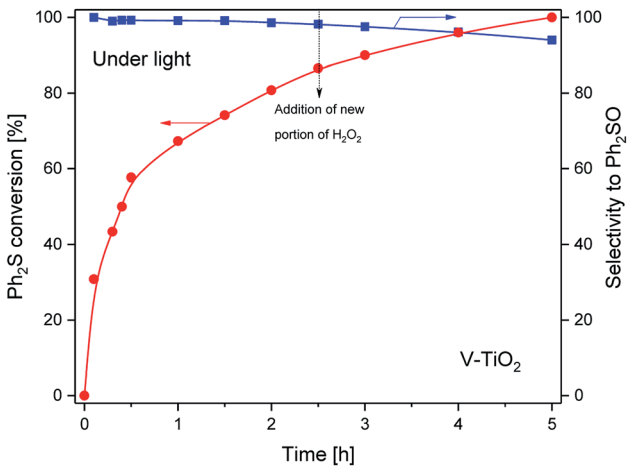

Fig. 8 Results of photocatalytic (under light) diphenyl sulphide oxidation by H_2O_2 in the presence of the V-TiO_2 sample. After 2.5 h of the test a new additional portion of H_2O_2 was added.

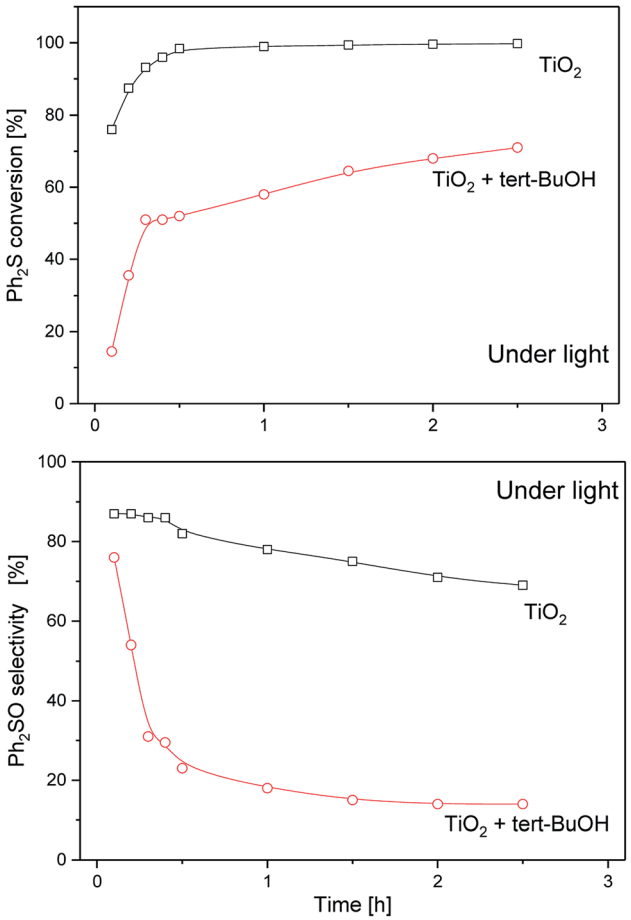

Fig. 9 Results of the photocatalytic conversion of diphenyl sulphide oxidation by H_2O_2 in the presence of the TiO_2 (P25) sample after the addition of a hydroxyl radicals scavenger (*t*-BuOH).

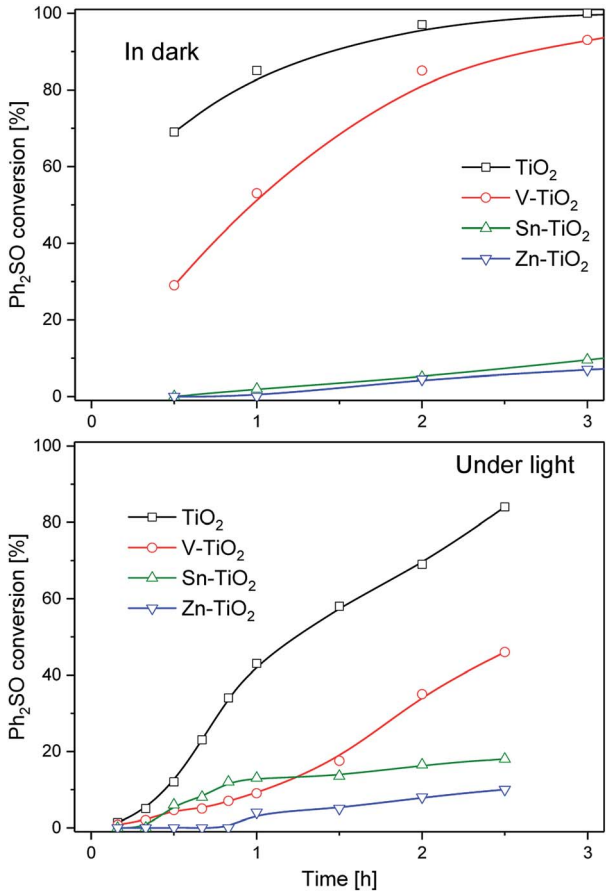

Fig. 10 Results of the oxidation of Ph_2SO to Ph_2SO_2 over TiO_2 and its modifications with metals in the dark (top) and under the light (bottom).

contain both anatase and rutile phases, while in Sn-TiO_2 and Zn-TiO_2 only the anatase phase was identified. Considering the significantly different catalytic performances of each catalysts, which follows the rutile content and very small amounts of the doping metals (about 0.1 wt%), it seems that the phase composition is the most important factor governing the catalytic and photocatalytic properties of the samples. The role of the deposited metals as phase composition controllers was very important for the phase transformations of TiO_2 (P25) during the calcination process.

The rutile containing samples, TiO_2 and V-TiO_2, presented much better catalytic activity in the dark compared with the samples that only contain the anatase phase, Sn-TiO_2 and Zn-TiO_2. It seems that rutile plays a crucial role in the second oxidation stage, $Ph_2SO \rightarrow Ph_2SO_2$, while anatase is significantly less active in this reaction (Fig. 10). In the case of the diphenyl sulphide oxidation upon irradiation, the best activity was found for calcined TiO_2, which contains both anatase and rutile components. A further increase in the rutile contribution, observed in the V-TiO_2 sample, decreased the efficiency of the photocatalytic diphenyl sulphide oxidation. Thus, the presence of both anatase and rutile phases, with their favourable contributions typical for P25, is necessary for the effective oxidation of Ph_2S to Ph_2SO. For the second oxidation stage the presence of rutile seems to be necessary to effectively catalyse the oxidation of Ph_2SO to Ph_2SO_2.

Conclusions

Zinc, tin and vanadium introduced into TiO_2 (P25) governed the phase transformations that occurred during its thermal treatment (550 °C/6 h). For TiO_2 and its vanadium-doped form (V-TiO_2), thermal treatment resulted in a decrease of the anatase and an increase of the rutile content in comparison with non-calcined P25. This effect is possibly related to the location of V^{4+} cations in the Ti^{4+} vacancies in the anatase lattice and therefore to the initiation of the anatase to rutile phase transformation. The opposite effect was observed for TiO_2 doped with zinc or tin, where thermal treatment resulted in the complete rutile to anatase phase transition. The ionic radii of Zn^{2+} and Sn^{4+} are too large to substitute Ti^{4+} in the anatase lattice and therefore the possible initiation of the anatase to rutile phase transformation was not observed.

The TiO_2 samples doped with vanadium, zinc, or tin were tested as catalysts and photocatalysts for diphenyl sulphide

oxidation to diphenyl sulfoxide and diphenyl sulfone using hydrogen peroxide as an oxidation agent. The differences in catalytic and photocatalytic activity were more due to the content of the rutile and anatase phases in the samples than to the introduced V, Zn and Sn admixtures. The catalysts containing rutile, TiO_2 and V-TiO_2, were significantly more active in diphenyl sulphide oxidation than the catalysts that only contained the anatase phase, Sn-TiO_2 and Zn-TiO_2. In the case of TiO_2 and V-TiO_2, both oxidation products, diphenyl sulfoxide and sulfone, were formed with significant contributions; while in the case of Sn-TiO_2 and Zn-TiO_2 the selectivity towards diphenyl sulfoxide dominated over the selectivity towards diphenyl sulfone. The efficiency of diphenyl sulphide oxidation increased under UV radiation. The best photocatalytic activity was for the sample containing both anatase and rutile (TiO_2). For the V-TiO_2 sample, with increased rutile content, a decrease in the efficiency of photocatalytic diphenyl sulphide oxidation was observed. Also, the Sn-TiO_2 and Zn-TiO_2 samples, only containing the anatase phase, presented lower photocatalytic activity than calcined TiO_2. Thus, the presence of both anatase and rutile phases, with their favourable contributions typical for P25, is necessary for the effective oxidation of Ph_2S to Ph_2SO. It was shown that rutile plays a crucial role in the second oxidation stage, Ph_2SO to Ph_2SO_2, while anatase is less active in this reaction.

Conflicts of interest

There are no conflicts to declare.

Acknowledgements

The work was supported by the Foundation for Polish Science (FNP) within the TEAM project (POIR.04.04.00-00-3D74/16). Part of the research was carried out with the equipment purchased thanks to the financial support of the European Regional Development Fund in the framework of the Polish Innovation Economy Operational Program (contract no. POIG.02.01.00-12-023/08).

References

1 W. Al-Maksoud, S. Daniele and A. B. Sorokin, *Green Chem.*, 2008, **10**, 447–451.
2 M. B. Smith and J. March, March's advanced organic chemistry, *Oxidations and reductions*, Wiley, New York, 6th edn, 2007, pp. 1780–1783.
3 B. M. Trost, *Science*, 1991, **254**, 1471–1477.
4 J. Přech, R. E. Morris and J. Čejka, *Catal. Sci. Technol.*, 2006, **6**, 2775–2786.
5 A. Shaabani and A. H. Rezayan, *Catal. Commun.*, 2007, **8**, 1112–1116.
6 H. Golchoubian and F. Hosseinpoor, *Molecules*, 2007, **12**, 304–311.
7 K. Sato, M. Hyodo, M. Aoki, X.-Q. Zheng and R. Noyori, *Tetrahedron*, 2001, **57**, 2469–2476.
8 R. Noyori, M. Aoki and K. Sato, *Chem. Commun.*, 2003, 1977–1986.
9 Y.-W. Chen, J.-Y. Chang and B. Moongraksathum, *J. Taiwan Inst. Chem. Eng.*, 2015, **52**, 140–146.
10 A. Di Paola, E. García-López, S. Ikeda, G. Marcí, B. Ohtani and L. Palmisano, *Catal. Today*, 2002, **75**, 87–93.
11 O. Carp, C. L. Huisman and A. Reller, *Prog. Solid State Chem.*, 2004, **32**, 33–177.
12 M. Bettinelli, V. Dallacasa, D. Falcomer, P. Fornasiero, V. Gombac, T. Montini, L. Romanò and A. Speghini, *J. Hazard. Mater.*, 2007, **146**, 529–534.
13 M. I. Litter and J. A. Navío, *J. Photochem. Photobiol., A*, 1994, **84**, 183–193.
14 K. Wilke and H. D. Breuer, *Z. Phys. Chem.*, 1999, **213**, 135–140.
15 S. M. Karvinen, *Ind. Eng. Chem. Res.*, 2003, **42**, 1035–1043.
16 M. Anpo, Y. Ichihashi, M. Takeuchi and H. Yamashita, *Res. Chem. Intermed.*, 1998, **24**, 143–149.
17 S. T. Martin, C. L. Morrison and M. R. Hoffmann, *J. Phys. Chem.*, 1994, **98**, 13695–13704.
18 P.-Y. Chang, C.-H. Huang and R. Doong, *Water Sci. Technol.*, 2009, **59**, 523–530.
19 W.-C. Lin and Y.-J. Lin, *Environ. Eng. Sci.*, 2012, **29**, 447–452.
20 H. Yamashita, M. Harada, J. Misaka, M. Takeuchi, B. Neppolian and M. Anpo, *Catal. Today*, 2003, **84**, 191–196.
21 H. Khan and D. Berk, *React. Kinet., Mech. Catal.*, 2014, **111**, 393–414.
22 M. Radko, A. Kowalczyk, E. Bidzińska, S. Witkowski, S. Górecka, D. Wierzbicki, K. Pamin and L. Chmielarz, *J. Therm. Anal. Calorim.*, 2018, **132**, 1471–1480.
23 M. Ferrari and L. Lutterotti, *J. Appl. Phys.*, 1994, **76**, 7246–7255.
24 M. Lubas, J. J. Jasinski, M. Sitarz, L. Kurpaska, P. Podsiad and J. Jasinski, *Spectrochim. Acta, Part A*, 2014, **133**, 867–871.
25 G. N. Shao, S.-J. Jeon, M. S. Haider, N. Abbass and H. T. Kim, *J. Colloid Interface Sci.*, 2016, **474**, 179–189.
26 N. Khatun, P. Rajput, D. Bhattacharya, S. N. Jha, S. Biring and S. Sen, *Ceram. Int.*, 2017, **43**, 14128–14134.
27 M. V. Martínez-Huerta, J. L. G. Fierro and M. A. Bañares, *Catal. Commun.*, 2009, **11**, 15–19.
28 M. A. Bañares, L. J. Alemany, M. C. Jiménez, M. A. Larrubia, F. Delgado, M. López Granados, A. Martínez-Arias, J. M. Blasco and J. L. G. Fierro, *J. Solid State Chem.*, 1996, **124**, 69–76.
29 W. Sangchay, *Energy Procedia*, 2016, **89**, 170–176.
30 M. Kobielusz, P. Mikrut and W. Macyk, *Adv. Inorg. Chem.*, 2018, **72**, 93–144.
31 M. Surówka, M. Kobielusz, M. Trochowski, M. Buchalska, K. Kruczała, P. Broś and W. Macyk, *Appl. Catal., B*, 2019, **247**, 173–181.
32 M. Buchalska, M. Kobielusz, A. Matuszek, M. Pacia, S. Wojtyła and W. Macyk, *ACS Catal.*, 2015, **5**, 7424–7431.
33 M. R. Hoffmann, S. T. Martin, W. Y. Choi and D. W. Bahnemann, *Chem. Rev.*, 1995, **95**, 69–96.
34 A. Mills and S. L. Hunte, *J. Photochem. Photobiol., A*, 1997, **108**, 1–35.
35 P. Zhang, Y. Wang, H. Li and M. Antonietti, *Green Chem.*, 2012, **14**, 1904–1908.